APPENDIX E

HORIZONTAL ANISOTROPY (RESPONSE TO USFIC 5.01)

Note Regarding the Status of Supporting Technical Information

This document was prepared using the most current information available at the time of its development. This Technical Basis Document and its appendices providing Key Technical Issue Agreement responses that were prepared using preliminary or draft information reflect the status of the Yucca Mountain Project's scientific and design bases at the time of submittal. In some cases this involved the use of draft Analysis and Model Reports (AMRs) and other draft references whose contents may change with time. Information that evolves through subsequent revisions of the AMRs and other references will be reflected in the License Application (LA) as the approved analyses of record at the time of LA submittal. Consequently, the Project will not routinely update either this Technical Basis Document or its Key Technical Issue Agreement appendices to reflect changes in the supporting references prior to submittal of the LA.

APPENDIX E

HORIZONTAL ANISOTROPY (RESPONSE TO USFIC 5.01)

This appendix provides a response for Key Technical Issue (KTI) agreement Unsaturated and Saturated Flow Under Isothermal Conditions (USFIC) 5.01. This KTI agreement relates to providing more information about horizontal anisotropy in the volcanic tuff.

E.1 KEY TECHNICAL ISSUE AGREEMENT

E.1.1 USFIC 5.01

KTI agreement USFIC 5.01 was reached during the U.S. Nuclear Regulatory Commission (NRC)/U.S. Department of Energy (DOE) technical exchange and management meeting on unsaturated and saturated flow under isothermal conditions held October 31 through November 2, 2000, in Albuquerque, New Mexico. The saturated zone portion of KTI subissues 5 and 6 were discussed at that meeting (Reamer and Williams 2000).

During the technical exchange, the NRC and the DOE discussed the appropriate degree of anisotropy for the site-scale saturated zone flow model (SSFM), the calibration of the model, and the use of alternative conceptual models. The DOE asserted that the isotropic case is really anisotropic, given the discrete features, such as faults, included in the SSFM. The NRC asked if the calibration was based on the isotropic or anisotropic case, to which the DOE replied that calibration was performed with the isotropic case. Following the discussion, agreement USFIC 5.01 was reached to perform additional evaluation of anisotropy.

Wording of the agreement is:

USFIC 5.01

> Anisotropy in the site scale model should be reevaluated to ensure that a reasonable range for uncertainty is captured. The data from the C-Wells testing should provide a technical basis for an improved range. As part of the C-Wells report, DOE should include an analysis of horizontal anisotropy for wells that responded to the long-term tests. Results should be included for the tuffs in the calibrated site scale model. DOE will provide the results of the requested analyses in C-Wells report(s) in October 2001, and will carry the results forward to the site-scale model, as appropriate.

E.1.2 Related Key Technical Issues

None.

E.2 RELEVANCE TO REPOSITORY PERFORMANCE

The subject of USFIC 5.01 is the further evaluation of the effects of anisotropy on model performance. This is directly relevant to the sensitivity of parameter uncertainty on model output and, subsequently, performance assessment.

Because potential radionuclides released from the repository must travel through the saturated fractured tuff and the saturated alluvium before reaching the compliance boundary, it is important to characterize the hydrogeologic properties of the downgradient media. In these volcanic tuffs, fractures and faults often have common orientations and it is likely that preferential flowpaths exist along these features. Anisotropy in hydraulic properties of the volcanic tuffs affects uncertainty in flow paths. Large-scale anisotropy and heterogeneity were implemented in the SSFM through direct incorporation of known hydraulic features, faults, and fractures. Small-scale anisotropy was derived from the analysis of hydraulic testing at the C-Wells (BSC 2003a, Section 6.2.6).

Additional analysis of anisotropy was needed for the SSFM for proper calibration of the model and for the use of alternative conceptual models. If uncertainty is large, with a range that could extend from an isotropic model to an anisotropic model, model prediction results could be different.

E.3 RESPONSE

Since completion of the C-Wells complex in 1983, several single and cross-hole tracer and hydraulic tests have been conducted to gain a better understanding of the hydrogeology of the region. The purpose of the testing was to characterize the hydrologic properties of the saturated zone at and around Yucca Mountain. Data from the testing were used for a more detailed analysis of anisotropy than the analyses originally performed. Although data from the C-Wells tests were not intended to be used for an analysis of anisotropy, an estimate of the anisotropy ratio could be made because drawdown was measurable at several distant wells (BSC 2003a, Section 6.2.6). Based on this analysis, a wider range of horizontal anisotropy than was used in the site recommendation was considered for the license application. Sensitivity analyses using the SSFM indicated that variation in anisotropy affected flow path lengths in the volcanic tuffs and alluvium.

The information in this report is responsive to agreement USFIC 5.01 made between the DOE and NRC. The report contains the information that DOE considers necessary for the NRC to review for closure of this agreement.

E.4 BASIS FOR THE RESPONSE

Because radionuclides released from the repository would have to travel through the saturated fractured tuff and the saturated alluvium before reaching the compliance boundary, it is important to characterize the hydrogeologic properties of downgradient media and their effects on saturated zone flow and radionuclide transport. In the volcanic tuffs, fractures and faults often have common orientations, and it is likely that preferential flowpaths exist along these features. A number of published studies have assigned transmissivities, storativities, and anisotropy ratios to the saturated zone in this area. In this analysis, reviews of several studies are

used in conjunction with an independent re-analysis of the data to derive a distribution of anisotropy ratios ranging from 0.05 to 20 for use in the site-scale saturated zone flow code (i.e., FEHM; (LANL 2003)).

E.4.1 Background of the Site-Scale Flow Models

In general, large-scale hydraulic features (e.g., major faults, fault zones, and zones of chemical alteration) have been incorporated into models as zones of enhanced or reduced permeability. However, the area of fractured volcanic tuffs beneath and downgradient to the south and east of the repository area (Figure E-1, Table E-1) is assigned stochastically-selected horizontal anisotropy values, which is the focus of this appendix. Originally, this area was represented in the conceptual model as isotropic, and horizontal anisotropy in permeability was considered an alternative conceptual model. For the total system performance assessment for the site recommendation (CRWMS M&O 2000a), two models were examined to evaluate the effect of uncertainty in anisotropy: an isotropic case and an anisotropic case with a 5:1 north–south anisotropy ratio. When calibrating the total system performance assessment for the site recommendation model (CRWMS M&O 2000a), a slightly better match to water level data was achieved when a 5:1 north–south anisotropy ratio was used. In addition, differences in predicted heads and the effects on specific discharge, flow-path direction, and flow-path lengths in volcanic tuffs and alluvium were within the uncertainty ranges in the total system performance assessment for the site recommendation (CRWMS M&O 2000a). Although only minor differences in model performance were recorded between the isotropic and 5:1 north–south anisotropic cases, it was felt that these discrete values were not representative of the system. Since then, a more detailed analysis of anisotropy has been performed. The results were presented in the *Saturated Zone In-Situ Testing* report (BSC 2003a, Section 6.2.6), and they were used in site-scale saturated zone flow and transport model abstractions (BSC 2003b, Section 6.5.2.10).

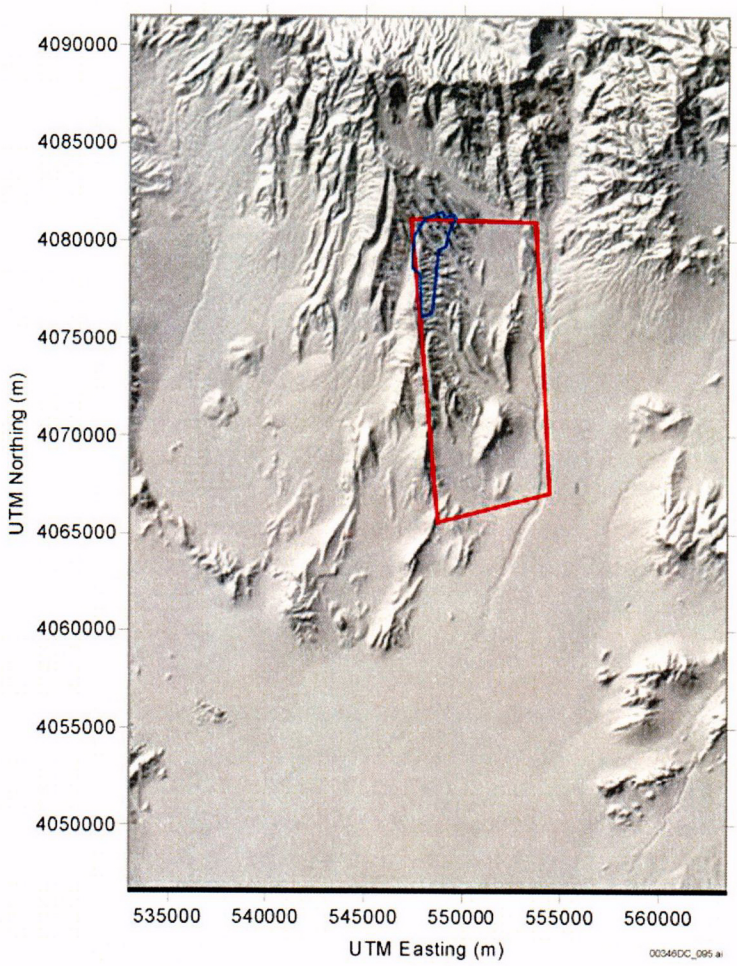

Source: DTN: SN0306T0502103.008.

Figure E-1. Horizontal Anisotropy Uncertainty Zone

Table E-1. Boundaries of the Horizontal Anisotropy Uncertainty Zone

Vertex	UTM Easting(m)	UTM Northing (m)
1	548712	4065570
2	554390	4067050
3	553647	4080900
4	547317	4081090

DTN: SN0306T0502103.008.

E.4.2 Analyses of Data from the C-Wells

A geologic description of the C-Wells complex and the surrounding area is presented elsewhere (e.g., Geldon et al. 1998; Farrell et al. 1999; Ferrill et al. 1999; Winterle and La Femina 1999; CRWMS M&O 2000b; BSC 2003a). Furthermore, a detailed description of the analysis and derivation of the distribution of the anisotropy ratio in the saturated zone near the C-Wells complex is presented in BSC (2003a, Section 6.2.6). Borehole logs for the C-Wells are shown in

Figure E-2. Interpretation of well-test data with analytical solutions consists of inferring the hydraulic properties of a system based on measured responses to an assumed flow geometry (i.e., radial). The system geometry cannot be specified with reasonable certainty. In a layered sedimentary system lacking extreme heterogeneity, flow might be expected to be radial during a hydraulic test. However, when hydraulic tests are conducted at an arbitrary point within a three-dimensional fractured rock mass, the flow geometry is complex (Hsieh et al. 1985). Radial flow would occur only if the test were performed in a single uniform fracture of effectively infinite extent or within a network of fractures confined to a planar body in which the fractures were so densely interconnected that the network behaves like an equivalent porous medium. Flow in fractured tuff is nonradial and variable, as fracture terminations and fracture intersections are reached by the cone of depression. Therefore, assumptions required in the analytical treatment of anisotropy may not be strictly consistent with site geology.

There is heterogeneity in hydraulic properties throughout the fractured tuff and alluvium near Yucca Mountain, which differ spatially and differ depending on the direction in which they are measured (horizontally and vertically). In this analysis, transmissivity and storativity are required to calculate and define large-scale anisotropy, and the measured values reflect heterogeneity in the media. The concept of anisotropy typically is associated with homogeneous medium, a criterion not met here. Nevertheless, there are spatial and directional variations in transmissivity, and the notion remains that, over a large enough representative elementary volume, there exists a preferential flow direction that can be termed "anisotropy." Structural features (e.g., fractures and faults) are indirectly incorporated into the anisotropy ratio applied to this area through the anisotropy analysis that considered the media as a homogeneous representative elementary volume.

Data from a long-term pumping test (May 8, 1996, to November 12, 1997) were used to evaluate anisotropy near the C-Wells complex. For this test, the most productive portion of the Bullfrog-Tram lithologic interval in borehole UE-25 c#3 was isolated with downhole packers, and water levels were monitored at several distant boreholes (USW-H4, UE-25 ONC#1, UE-25 WT#3, and UE-25 WT#14). Data from the other C-Wells (UE-25 c#1 and UE-25 c#2) were not used in the anisotropy analysis because over the small scale of observation at the C-Wells pump test results likely are dominated by discrete fractures (i.e., inhomogeneities), three-dimensional flow effects are likely, and recirculation from simultaneous tracer tests obscured the results. Furthermore, because anisotropy is conceptually difficult to define for heterogeneous media, it is more easily described as an average preferential flow over as large a representative elementary volume as possible. Thus, it makes little sense to define anisotropy over a heterogeneous area as small as that of the C-Wells complex. The nonradial nature of the cone of depression near the C-Wells is illustrated in Figure E-3. After filtering (USGS 2002) the drawdown data in response to pumping at UE-25 c#3, transmissivity and storativity were calculated at four distant wells (USW H-4, UE-25 ONC#1, UE-25 WT#3, and UE-25 WT#14). Figure E-4 is a plot of the filtered drawdowns fit with the Cooper-Jacob straight-line method (CRWMS M&O 2000c). The inconsistent slope of the fit to drawdown in well USW H-4 resulted in a lower transmissivity at this well, which could be due to the Antler Wash fault that runs north-northeast between wells UE–25 c#3 and USW H–4. Transmissivity and storativity values are presented in Table E-2. The variations in transmissivity and storativity support the alternative conceptual model in which there is large-scale horizontal anisotropy in permeability in the saturated zone volcanic units southeast of the repository.

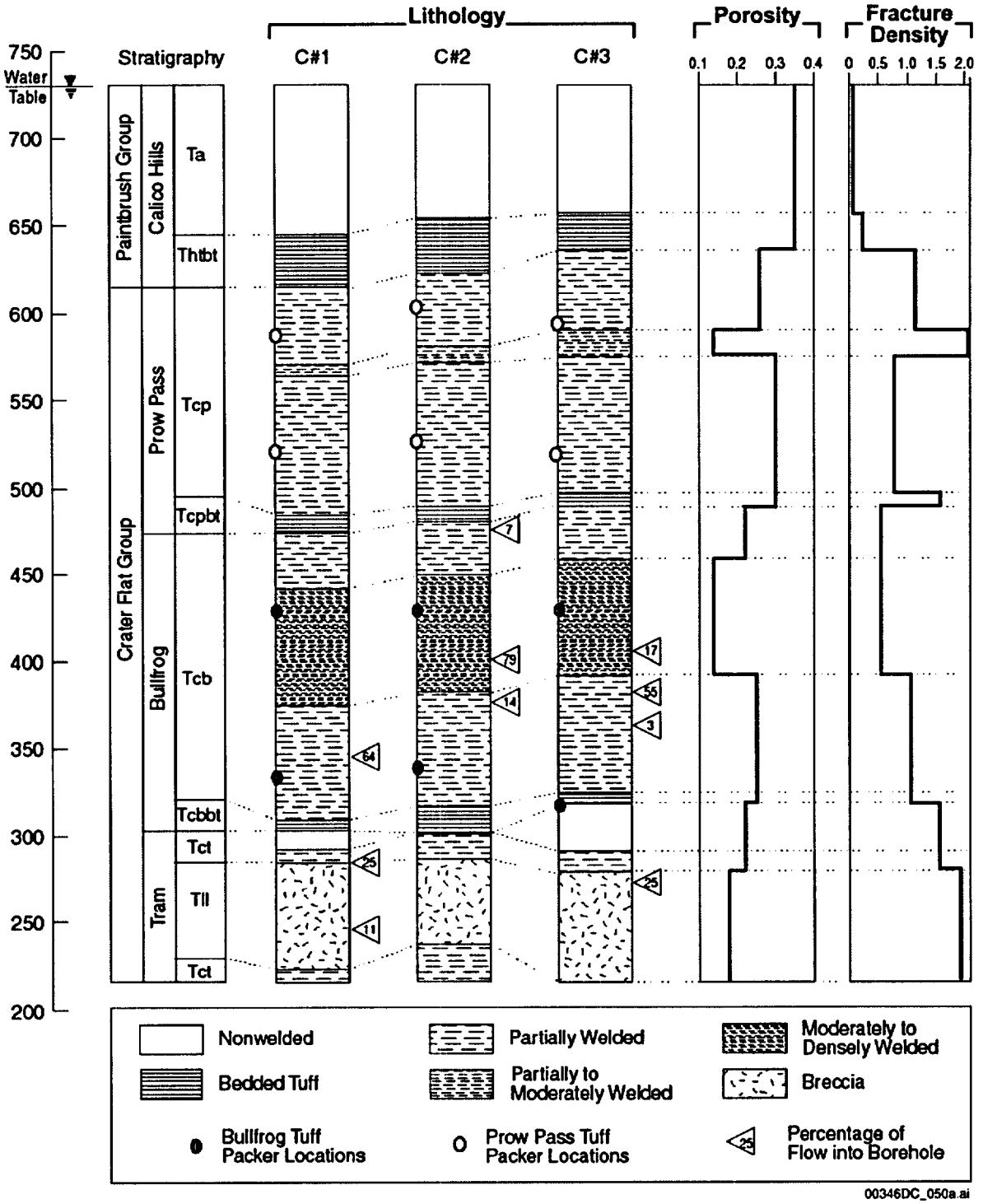

Source: Information derived from Geldon 1993, pp. 35–37, 68–70. Packer locations from Umari 2002.

NOTE: Packer locations indicate intervals in which tracer tests described in this report were conducted. The tracer tests were conducted between UE-25 c#2 and UE-25 c#3.

Figure E-2. Stratigraphy, Lithology, Matrix Porosity, Fracture Density, and Inflow from Open-Hole Flow Surveys at the C-Wells

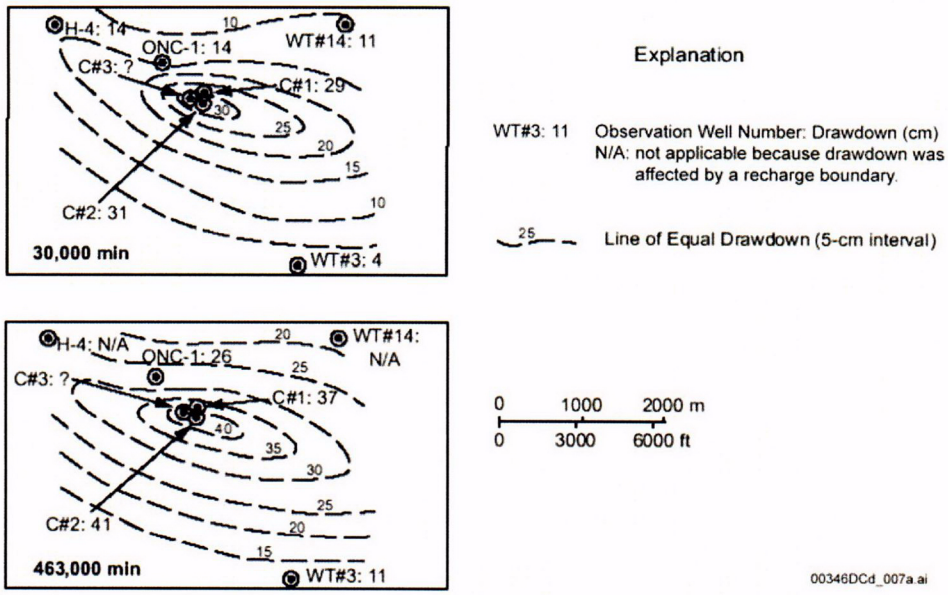

Source: BSC 2003a, Figure 6.2-36.

NOTE: The upper panel shows the distribution 30,000 min (20.8 days) after pumping started; the lower panel shows the distribution 463,000 min (321.5 days) after pumping started.

Figure E-3. Non-Radial Cones of Depression near the C-Wells at Two Times after Pumping Started in UE-25 c#3

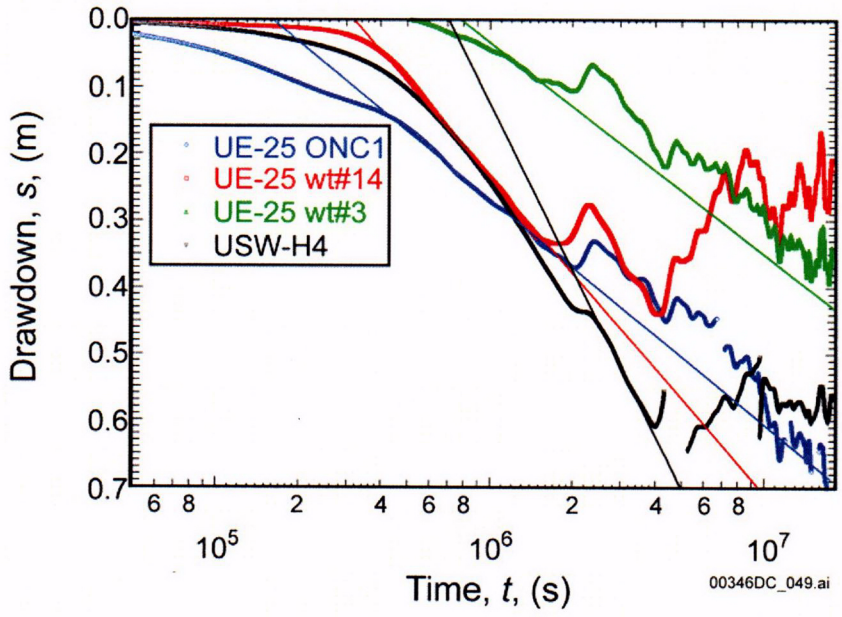

Source: BSC 2003a, Figure 6.2-39.

Figure E-4. Linear Fits to Filtered Data from Four Monitoring Wells

COZ

Table E-2. Transmissivities and Storativities Calculated Using the Cooper-Jacob Method with Filtered Data

Well	Transmissivity (m^2/day)	Storativity
UE-25 ONC#-1	446	0.003
UE-25 WT#3	477	0.0005
UE-25 WT#14	318	0.0008
USW H-4	182	0.0007

Source: BSC 2003a.

E.4.3 Previously Reported Results

Winterle and La Femina (1999) processed long-term pumping data with AQTESOLV, and their transmissivity and storativity results (obtained with the Theis method) are shown in Table E-3. *Saturated Zone In-Situ Testing* (BSC 2003a) also analyzed the drawdown data from the long-term pumping test using the analytical methods of Theis (1935), Neuman (1975), and Streltsova-Adams (1978), and these results also are presented in Table E-3. There are obvious discrepancies between the results presented in Tables E-2 and E-3. Such variability is not surprising considering the differences in data reduction methods and solution techniques.

Table E-3. Transmissivities and Storativities of Distant Wells for the Long Term Pumping Tests

	Winterle and La Femina [a]		Geldon et al. [b]	
Well	Transmissivity (m^2/day)	Storativity	Transmissivity (m^2/day)	Storativity
UE-25 ONC#1	1,340	0.008	1,000	0.001
UE-25 WT#3	1,230	0.005	2,600	0.002
UE-25 WT#14	1,330	0.002	1,300	0.002
USW-H4	670	0.002	700	0.002

Source: BSC 2003a, Table 6.2-11.

NOTES: [a] Winterle and La Femina (1999)
[b] Geldon et al. (2002).

E.4.4 Anisotropy Ratios

Anisotropy ratio analyses (BSC 2003a) used the analytical solutions of Papadopulos (1967) combined with PEST (Watermark Computing 2002), hereafter referred to as the Papadopulos-PEST method, and Hantush (1966), both implemented with standard formulas of ellipses and coordinate transformations. Both techniques are applicable to homogeneous confined aquifers with radial flow to the pumping well, although small deviations from these assumptions may yield reasonable estimates of anisotropy. These methods require transmissivity, storativity, and the locations of at least three monitoring wells as input. Anisotropy ratios and principle directions are calculated from these data. Results from three analyses are presented in Table E-4.

Table E-4. Calculated and Reported Anisotropies and Principle Directions

Data Set Used	T_{max} (m^2/day)	T_{min} (m^2/day)	Anisotropy	Azimuth
BSC (2003a); Hantush (1966)	748	229	3.3	15°E
BSC (2003a) *T*=1,000 m^2/day (Papadopulos-PEST)	1,863	537	3.5	79°W
BSC (2003a) *T*=700–2,600 m^2/day (Papadopulos-PEST)	3,272	599	5.5	1°E
BSC (2003a) T=700–1,230 m^2/day (Papadopulos-PEST)	3,047	271	11.3	35°W
Ferrill et al. (1999)	5,400	315	17	30°E
Winterle and La Femina (1999)	2,900	580	5	33°E

Source: BSC 2003a, Table 6.2-12.

NOTE: *T* = transmissivity

E.4.5 Interpretation and Assignment of the Anisotropy Distribution

A distribution of anisotropies was specified so that an anisotropy ratio can be selected for each stochastic realization of the saturated zone flow and transport abstraction model (BSC 2003b). Because the current version of FEHM (LANL 2003) can only implement anisotropy aligned with the grid direction, the north-northeasterly principal direction is not directly implemented in the model, which further increases uncertainty. For example, the analytical result for anisotropy using the Cooper-Jacob (1946) method is a ratio of 3.3 in a direction 15° east of north. A projection that orients the principal direction north–south (0°) results in an anisotropy ratio of 2.5, and depending on the principle direction, it is possible for the projected north–south anisotropy ratio to be less than one.

To reflect uncertainty in the anisotropy data near the C-Wells, a relatively large range of anisotropies (large uncertainty) was used in the flow and transport abstraction models. All authors who have previously investigated anisotropy ratios in this area (Farrell et al. 1999; Ferrill et al. 1999; Winterle and La Femina 1999) agree that the assumptions made in the anisotropy analysis are difficult to support and that the analysis is sensitive to the input parameters. Reported anisotropies range from 3.3 (BSC 2003a, Table 6.2-12) to 17 (Ferrill et al. 1999), but "because of the considerable degree of uncertainty in the anisotropy ratio and direction obtained from [these analyses], the degree of confidence in [the] horizontal anisotropy analysis should be regarded as low" (Winterle and La Femina 1999, p. 4-25). Based on the ratio of a maximum of 3,800 m^2/day (Winterle and La Femina 1999, p. 4-12) to a minimum calculated transmissivity of 182 m^2/day (BSC 2003a, Table 6.2-10), and on the highest reported anisotropy ratio of 17 (Ferrill et al. 1999), the upper limit of the distribution of the projected north–south anisotropy ratio was conservatively set at 20. Although most anisotropy calculations and geologic interpretations report the direction of maximum principal hydraulic conductivity as approximately north-northeast, it cannot be ruled out that the direction of anisotropy could lie in the east–west direction (BSC 2003a, Table 6.2-12), causing the projected north–south to east–west anisotropy ratio to be less than 1. Therefore, the lower limit was set as the inverse of the upper limit, 1/20 or 0.05. This lower limit on anisotropy ratio is consistent with the Antler Wash fault found near the C-Wells complex. Thus, a small (10 percent) probability of the projected north–south to east–west anisotropy being less than 1 was assigned. Because 3 of 6 anisotropy analyses yielded ratios of anisotropy between 1 and 5 (BSC 2003a, Table 6.2-12), a 50 percent probability for the projected north south to east–west anisotropy ratio falling between 1 and 5

was assigned. This left a 40 percent probability of projected anisotropy ratios between 5 and 20. The resulting cumulative distribution function is shown in Figure E-5. For the SSFM, it is only possible to specify "projected" anisotropies in the north–south or east–west directions (independent of calculated principal direction), further justifying the large range of anisotropies.

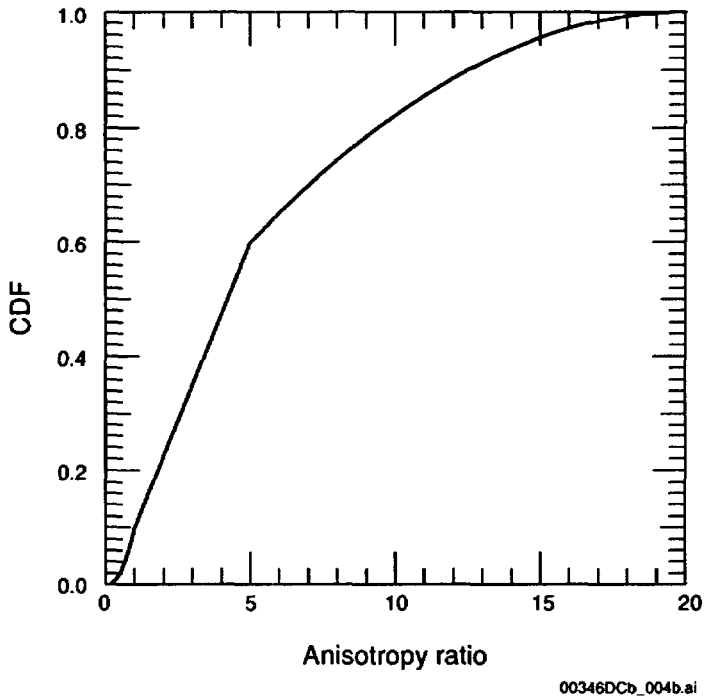

Source: BSC 2003b, Figure 6-19.

Figure E-5. Cumulative Distribution of Anisotropy Ratio

There are several noteworthy points based on three distinct regions of the anisotropy ratio distribution:

Anisotropy Ratio Between 5 and 20–The maximum anisotropy ratio of 20:1 is based on the highest reported anisotropy ratio 17:1 (Ferrill et al. 1999). To be conservative, the maximum reported value of 17:1 was rounded to 20:1 and set as the upper limit for horizontal anisotropy. Furthermore, although features such as high transmissivity zones and fractures may yield large local anisotropy ratios, their effects are globally attenuated and 20 is a reasonable maximum. The 5.5 anisotropy ratio calculated by the second approach of the modified Papadopulos-PEST method (BSC 2003a, Table 6.2-12) lies in this range. Therefore, between 5 and 20, a triangularly distributed anisotropy ratio was constructed that decreases to zero probability at 20. A 40 percent probability was assigned to this portion of the probability density function.

Anisotropy Ratio Between 0.05 and 1–Based on the existence of the Antler Wash fault and the uncertainty associated with the projected anisotropy discussed above, it is possible the media could be isotropic, and there is a small probability that the principal direction could be east–west.

Correspondingly, a north–south anisotropy ratio of less than 1 is possible, and the minimum anisotropy ratio was set equal to the inverse of the maximum, 1:20, with a triangularly distributed 10 percent probability decreasing to zero at a ratio of 0.05. One Papadopulos solution, yielding an anisotropy ratio of 3.5 at 79° west of north falls in this range (BSC 2003a).

Anisotropy Ratio Between 1 and 5–A uniformly distributed 50 percent probability is assigned to the range of anisotropy ratio between 1 and 5. This interval comprises the more likely values of anisotropy ratios with no specific value likely than another. In addition, in the total system performance assessment for the site recommendation model (CRWMS M&O 2000a) of the saturated zone near Yucca Mountain, anisotropy was binomially distributed with a 50 percent probability of isotropy (1:1) and a 50 percent probability of a 5:1 ratio (CRWMS M&O 2000a).

Based on a reevaluation of horizontal anisotropy in the SSFM using a reinterpretation of the C-Wells testing data, Figure E-5 is the best estimate for the cumulative distribution of north–south anisotropy ratios in the saturated zone used as stochastic input to FEHM (LANL 2003) in the saturated zone flow and transport abstractions (BSC 2003b).

E.4.6 Effects on Flow Path Length

There is variation in the simulated flow paths (BSC 2003b) over the range of uncertainty in the horizontal anisotropy in permeability considered in the model (Figure E-6). The uncertainty distribution for horizontal anisotropy assigns 90 percent probability to a value of greater than 1 for the ratio of north–south to east–west permeability, and consequently, the most likely flow paths are to the west of the blue particle paths shown in Figure E-6.

E.4.7 FEHM Model Sensitivity Study

An analysis of the sensitivity of head measurements (modeled using the SSFM; FEHM code) to changes in the anisotropy ratio revealed that the modeled heads were slightly sensitive to the anisotropy ratio. Figure E-7 illustrates how varying the anisotropy ratio affects the weighted root-mean-square error between measured and FEHM modeled heads. The root-mean-square error ranges between 6.9 and 7.6. Although this short range demonstrates relative insensitivity of the modeled heads to the anisotropy ratio, it is encouraging that the root-mean-square error decreases for anisotropy ratios between 0.05 to 20 and then subsequently increases.

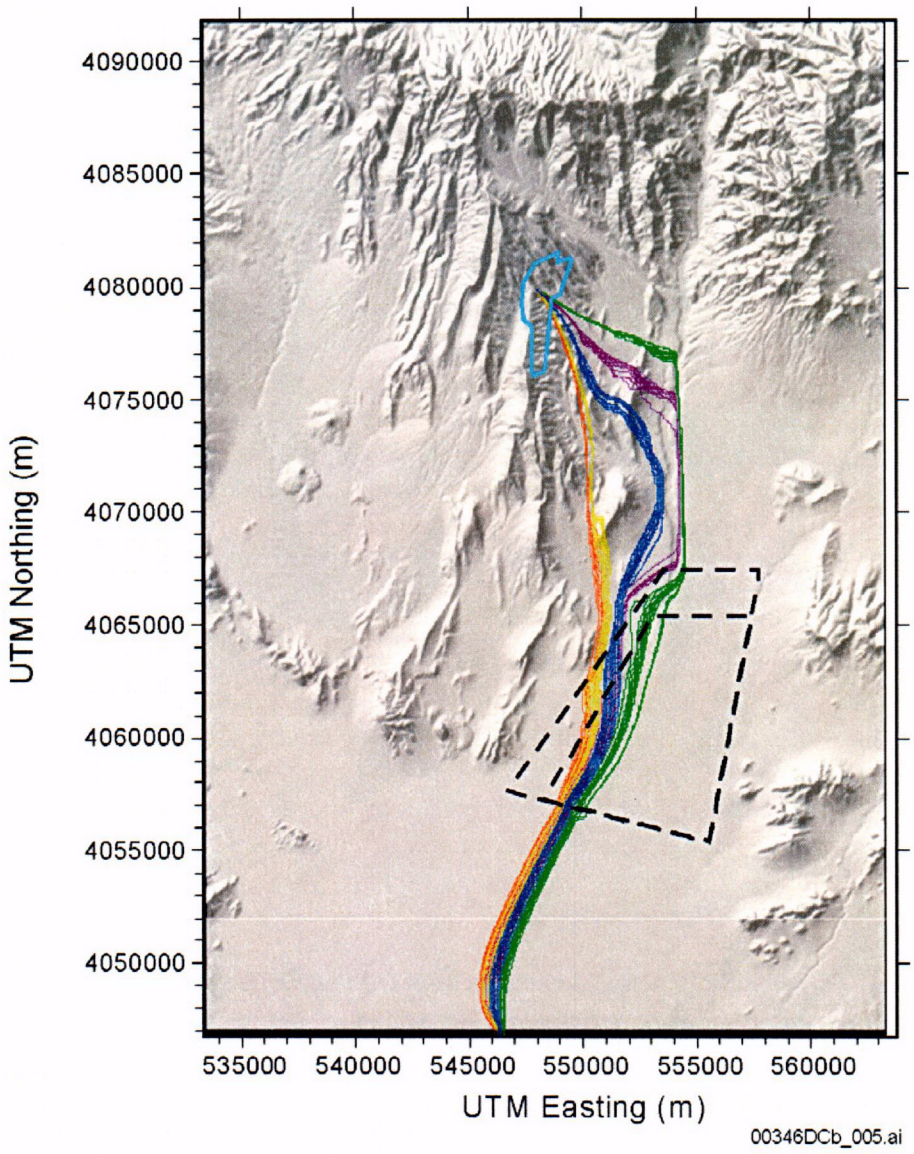

Source: Repository outline: BSC 2003c; alluvial uncertainty zone: BSC 2003b.

NOTE: Green, purple, blue, yellow, and red lines show simulated particle paths for horizontal anisotropy values of 0.05, 0.20, 1.0, 5.0, and 20.0, respectively. The dashed lines show the minimum and maximum boundaries of the alluvial uncertainty zone.

Figure E-6. Simulated Particle Paths for Different Values of Horizontal Anisotropy in Permeability

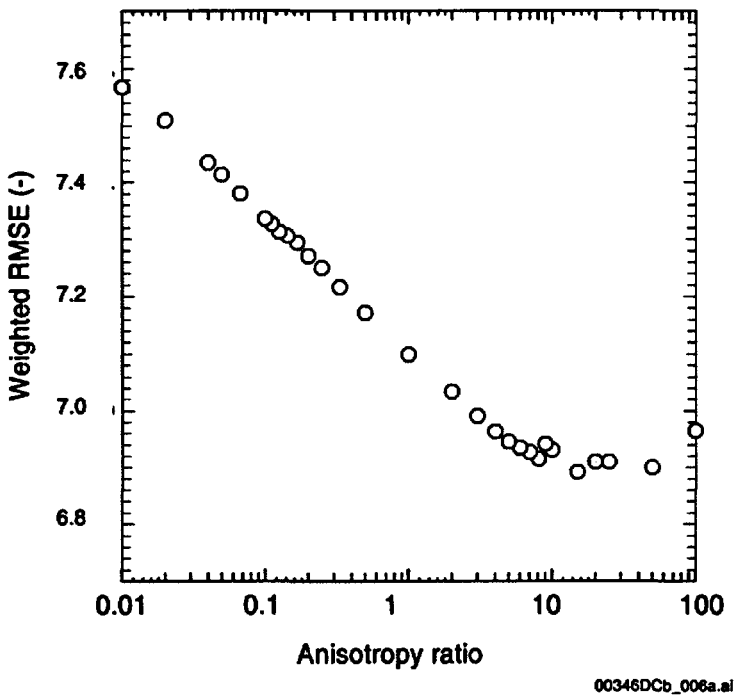

NOTE: RMSE = root-mean-square error. Data points are weighted RMSE between measured heads and FEHM-modeled heads over a range of anisotropy ratios.

Figure E-7. Sensitivity of Head Measurements to Changes in the Anisotropy Ratio

Although analytical and graphical techniques yield a single, specific anisotropy ratio, this value is sensitive to the solution technique and interpretations of the data by the analyst (e.g., assumptions, filtering parameters, and how the slopes of drawdown were calculated). A wide distribution of anisotropy ratios is suggested to account for the uncertainty in this hydrogeologic property. Each run of FEHM must have a single value of anisotropy assigned to the appropriate zone, and although this is unrealistic (no single value of anisotropy truly applies to such a large heterogeneous area), drawing an anisotropy ratio from the specified distribution and running FEHM stochastically effectively accounts for the uncertainty in this model parameter.

Field data were analyzed to identify anisotropy in flow direction. The data was used to derive an anisotropy distribution that will be used in total system performance assessment for the license application.

E.5 REFERENCES

E.5.1 Documents Cited

BSC (Bechtel SAIC Company) 2003a. *Saturated Zone In-Situ Testing.* ANL-NBS-HS-000039 REV 00A. Las Vegas, Nevada: Bechtel SAIC Company. ACC: MOL.20030602.0291.

BSC 2003b. *SZ Flow and Transport Model Abstraction.* MDL-NBS-HS-000021 REV 00A. Las Vegas, Nevada: Bechtel SAIC Company. ACC: MOL.20030612.0138.

BSC 2003c. *Repository Design, Repository/PA IED Subsurface Facilities.* 800-IED-EBS0-00401-000-00C. Las Vegas, Nevada: Bechtel SAIC Company. ACC: ENG.20030303.0002.

Cooper, H.H., Jr. and Jacob, C.E. 1946. "A Generalized Graphical Method for Evaluating Formation Constants and Summarizing Well-Field History." *Transactions, American Geophysical Union, 27,* (IV), 526-534. Washington, D.C.: American Geophysical Union. TIC: 225279.

CRWMS M&O (Civilian Radioactive Waste Management System Management and Operating Contractor) 2000a. *Total System Performance Assessment for the Site Recommendation.* TDR-WIS-PA-000001 REV 00 ICN 01. Las Vegas, Nevada: CRWMS M&O. ACC: MOL.20001220.0045.

CRWMS M&O 2000b. *Saturated Zone Flow and Transport Process Model Report.* TDR-NBS-HS-000001 REV 00 ICN 02. Las Vegas, Nevada: CRWMS M&O. ACC: MOL.20001102.0067.

CRWMS M&O 2000c. *Development Plan for Engineered Barrier System Features, Events and Processes, and Degradation Modes Analysis.* Development Plan TDP-EBS-MD-000010 REV 02. Las Vegas, Nevada: CRWMS M&O. ACC: MOL.20000421.0225.

Farrell, D.A.; Armstrong, A.; Winterle, J.R.; Turner, D.R.; Ferrill, D.A.; Stamatakos, J.A.; Coleman, N.M.; Gray, M.B.; and Sandberg, S.K. 1999. *Structural Controls on Groundwater Flow in the Yucca Mountain Region.* San Antonio, Texas: Center for Nuclear Waste Regulatory Analyses. TIC: 254265.

Ferrill, D.A.; Winterle, J.; Wittmeyer, G.; Sims, D.; Colton, S.; Armstrong, A.; and Morris, A.P. 1999. "Stressed Rock Strains Groundwater at Yucca Mountain, Nevada." *GSA Today, 9,* (5), 1-8. Boulder, Colorado: Geological Society of America. TIC: 246229.

Geldon, A.L. 1993. *Preliminary Hydrogeologic Assessment of Boreholes UE-25c #1, UE-25c #2, and UE-25c #3, Yucca Mountain, Nye County, Nevada.* Water-Resources Investigations Report 92-4016. Denver, Colorado: U.S. Geological Survey. ACC: MOL.19960808.0136.

Geldon, A.L.; Umari, A.M.A.; Earle, J.D.; Fahy, M.F.; Gemmell, J.M.; and Darnell, J. 1998. *Analysis of a Multiple-Well Interference Test in Miocene Tuffaceous Rocks at the C-Hole Complex, May-June 1995, Yucca Mountain, Nye County, Nevada.* Water-Resources Investigations Report 97-4166. Denver, Colorado: U.S. Geological Survey. TIC: 236724.

Geldon, A.L.; Umari, A.M.A.; Fahy, M.F.; Earle, J.D.; Gemmell, J.M.; and Darnell, J. 2002. *Results of Hydraulic Tests in Miocene Tuffaceous Rocks at the C-Hole Complex, 1995 to 1997, Yucca Mountain, Nye County, Nevada.* Water-Resources Investigations Report 02-4141. Denver, Colorado: U.S. Geological Survey. TIC: 253755.

Hantush, M.S. 1966. "Analysis of Data from Pumping Tests in Anisotropic Aquifers." *Journal of Geophysical Research, 71*, (2), 421-426. (Washington, D.C.: American Geophysical Union). TIC: 225281.

Hsieh, P.A.; Neuman, S.P.; Stiles, G.K.; and Simpson, E.S. 1985. "Field Determination of the Three-Dimensional Hydraulic Conductivity Tensor of Anisotropic Media. 2. Methodology and Application to Fractured Rocks." *Water Resources Research, 21*, (11), 1667-1676. Washington, D.C.: American Geophysical Union. TIC: 254511.

LANL (Los Alamos National Laboratory) 2003. *Software Code: FEHM.* V2.20. SUN, PC. 10086-2.20-00.

Neuman, S.P. 1975. "Analysis of Pumping Test Data from Anisotropic Unconfined Aquifers Considering Delayed Gravity Response." *Water Resources Research, 11*, (2), 329-342. Washington, D.C.: American Geophysical Union. TIC: 222414.

Papadopulos, I.S. 1967. "Nonsteady Flow to a Well in an Infinite Anisotropic Aquifer." *Hydrology of Fractured Rocks, Proceedings of the Dubrovnik Symposium, October 1965. 1*, 21-31. Gentbrugge, (Belgium): Association Internationale d'Hydrologie Scientifique. TIC: 223152.

Reamer, C.W. and Williams, D.R. 2000. Summary Highlights of NRC/DOE Technical Exchange and Management Meeting on Unsaturated and Saturated Flow Under Isothermal Conditions. Meeting held August 16-17, 2000, Berkeley, California. Washington, D.C.: U.S. Nuclear Regulatory Commission. ACC: MOL.20001201.0072.

Streltsova-Adams, T.D. 1978. "Well Hydraulics in Heterogeneous Aquifer Formations." Volume 11 of *Advances in Hydroscience*. (Chow, V.T., ed.). Pages 357-423. (New York, New York: Academic Press). TIC: 225957.

Theis, C.V. 1935. "The Relation Between the Lowering of the Piezometric Surface and the Rate and Duration of Discharge of a Well Using Ground-Water Storage." *Transactions of the American Geophysical Union Sixteenth Annual Meeting, April 25 and 26, 1935, Washington, D.C.* Pages 519-524. Washington, D.C.: National Academy of Science, National Research Council. TIC: 223158.

Umari, M.J. 2002. Performing Various Hydraulic and Tracer Tests Using Prototype Pressure Transducer and Packer Assemblies. Scientific Notebook SN-USGS-SCI-036-V1. ACC: MOL.20020520.0364; MOL.20020520.0368; through; MOL.20020520.0382.

USGS (U.S. Geological Survey) 2002. *Software Code: Filter.vi.* V 1.0. PC, Windows 2000/NT 4.0/98. 10970-1.0-00.

Watermark Computing 2002. *Software Code: PEST.* V5.5. SUN, PC, Linux. 10289-5.5-00.

Winterle, J.R. and La Femina, P.C. 1999. *Review and Analysis of Hydraulic and Tracer Testing at the C-Holes Complex Near Yucca Mountain, Nevada.* San Antonio, Texas: Center for Nuclear Waste Regulatory Analyses. TIC: 246623.

E.5.2 Data, Listed by Data Tracking Number

SN0306T0502103.008. Updated Saturated Zone Transport Abstraction Model Inputs and Results. Submittal date: 06/12/2003.

APPENDIX F

^{14}C RESIDENCE TIME (RESPONSE TO USFIC 5.06)

Note Regarding the Status of Supporting Technical Information

This document was prepared using the most current information available at the time of its development. This Technical Basis Document and its appendices providing Key Technical Issue Agreement responses that were prepared using preliminary or draft information reflect the status of the Yucca Mountain Project's scientific and design bases at the time of submittal. In some cases this involved the use of draft Analysis and Model Reports (AMRs) and other draft references whose contents may change with time. Information that evolves through subsequent revisions of the AMRs and other references will be reflected in the License Application (LA) as the approved analyses of record at the time of LA submittal. Consequently, the Project will not routinely update either this Technical Basis Document or its Key Technical Issue Agreement appendices to reflect changes in the supporting references prior to submittal of the LA.

APPENDIX F

^{14}C RESIDENCE TIME (RESPONSE TO USFIC 5.06)

This appendix provides a response for Key Technical Issue (KTI) agreement Unsaturated and Saturated Flow under Isothermal Conditions (USFIC) 5.06. This KTI agreement relates to providing more information about groundwater flow directions based on residence time of naturally occurring carbon isotopes.

F.1 KEY TECHNICAL ISSUE AGREEMENT

F.1.1 USFIC 5.06

KTI agreement USFIC 5.06 was reached during the U.S. Nuclear Regulatory Commission (NRC)/U.S. Department of Energy (DOE) technical exchange and management meeting on unsaturated and saturated flow under isothermal conditions held October 31 through November 2, 2000, in Albuquerque, New Mexico. The saturated zone portion of KTI Subissues 5 and 6 were discussed at that meeting (Reamer and Williams 2000).

Wording of the agreement is:

USFIC 5.06

> Provide a technical basis for residence time (for example, using ^{14}C dating on organic carbon in groundwater from both tuffs and alluvium). DOE will provide the technical basis for residence time in an update to the Geochemical and Isotopic Constraints on Groundwater Flow Directions, Mixing, and Recharge at Yucca Mountain, Nevada AMR during FY 2002.

F.1.2 Related Key Technical Issue Agreements

None.

F.2 RELEVANCE TO REPOSITORY PERFORMANCE

Understanding and confirming groundwater flow paths and mixing zones using independent data sets is beneficial for ensuring that the results of predictive models can be relied on for the license application. Although advective transport properties are reasonably constrained by in situ observations from boreholes, these observations are limited by the time and space over which the testing was conducted. For example, the scale of the C-Wells and Alluvial Testing complexes are representative of spatial scales of tens of meters and temporal scales of days to months. The transport processes of relevance to repository performance occur over spatial scales of kilometers and temporal scales of thousands of years.

One of the few methods to investigate relevant transport processes over the spatial and temporal scale of interest to repository performance is the use of naturally occurring radioisotopes such as ^{14}C. The use of naturally occurring radioisotopes for assessing the flow of groundwater and

radionuclide transport in the saturated zone beneath and downgradient from Yucca Mountain is described in Section 3.2.3.

F.3 RESPONSE

The activity of ^{14}C has been measured (in percent modern carbon, pmc) in several boreholes in and adjacent to the site-scale model area). Most boreholes had less than 30 pmc, but there were a few notable exceptions in northern Fortymile Wash. The general trend of the data did not support decreasing ^{14}C along potential flow pathways from the proposed repository. The carbon reservoir (principally as bicarbonate) in groundwater is readily modified through reactions with aquifer rock along a flow pathway. Therefore, it is necessary to evaluate potential sources of carbon in the groundwater before using ^{14}C data to evaluate flow pathways or residence times.

Due to the nonconservative nature of carbon in groundwater, carbon isotopes are not used to evaluate flow pathways. Rather, the approach used was to evaluate potential flow pathways based on conservative species, principally chlorine and sulfate, in conjunction with the potentiometric surface map. After identifying potential flow paths, additional hydrochemical species were considered to evaluate whether they behave conservatively and are consistent with the flow paths, or if nonconservative behavior can be explained through reasonable chemical reactions. This iterative process resulted in determining the final potential flow paths. ^{14}C data from groundwater along the potential flow pathways were then evaluated to determine transport time. Measured ^{14}C activities were corrected to account for decreases in ^{14}C activity that resulted from water-rock interactions and the mixing of groundwaters, as identified by the PHREEQC mixing and chemical reaction models. This process resulted in estimates of decreases in ^{14}C activity due to radioactive decay during transit between boreholes, which can be converted into transit time using the radioactive decay equation (Equation F-1). After determining the transit time between boreholes, linear groundwater velocities were determined by dividing the distance between the boreholes by the transit time. In a similar fashion, ^{14}C activity was used to evaluate the range of ages of water and the components of young water present in areas thought to be dominated by local recharge.

Given the distribution of ages calculated for perched waters, an average residence time was in the range of 10,000 to 13,000 yr. This result is comparable with the range in ages (8,000 to 16,000 yr) calculated for saturated zone waters from ^{14}C measurements on dissolved organic ^{14}C.

^{13}C results suggest that groundwater under Yucca Mountain is not simply groundwater that flowed southward from recharge areas to the north (e.g., Timber Mountain), but represents local recharge at Yucca Mountain and in areas immediately to the north (e.g., Yucca Wash and Pinnacles Ridge).

The information in this report is responsive to agreement USFIC 5.06 made between the DOE and NRC. The report contains the information that DOE considers necessary for the NRC to review for closure of this agreement.

F.4 BASIS FOR THE RESPONSE

F.4.1 Identification of Flow Paths

Groundwater flow paths and mixing zones were identified based on measured and calculated geochemical and isotopic parameters. The hydraulic gradient, shown on the potentiometric surface map (BSC 2003, Figure 4), was used to constrain flow directions. Chemical and isotopic composition of groundwater was then used to locate flow pathways in the context of the hydraulic gradient, considering the possibility that flow paths can be oblique to the potentiometric gradient because of anisotropy in permeability.

The analysis of flow paths assumes that chloride (Cl^-) and sulfate (SO_4^{2-}) values are conservative and that changes to these species are due to mixing along flow paths. Flow paths can be traced using conservative constituents where compositional differences exist that allow some directions to be eliminated as possible flow directions. However, no single chemical or isotopic species varies sufficiently in the study area to determine flow paths everywhere. Therefore, multiple lines of evidence were used to construct flow paths, including the areal distribution of multiple chemical and isotopic species, potential sources of recharge, groundwater ages, and the evaluation of mixing and groundwater evolution through scatterplots and inverse mixing and reaction models.

Figure F-1 presents flow pathways inferred from hydrochemical data (Cl^- illustrated). Groundwater transport time, based on ^{14}C activities, was evaluated for specific samples along flow paths near the repository, as discussed below.

F.4.2 Carbon Isotopes in the Environment

Carbon has two stable isotopes (^{12}C and ^{13}C) and a third isotope, ^{14}C, which is radioactive. ^{14}C is produced in the atmosphere by a variety of nuclear reactions, the most important of which is the interaction of cosmic ray neutrons with ^{14}N. ^{14}C is rapidly mixed in the atmosphere and incorporated into carbon dioxide (CO_2) where it is then available for incorporation into terrestrial carbonaceous materials. The radioactive decay of ^{14}C, with a half-life of 5,730 years, forms the basis for radiocarbon dating. The ^{14}C age of a groundwater sample is calculated as

$$t = -\frac{1}{\lambda}\ln\left(\frac{^{14}A}{^{14}A_0}\right) \qquad \text{(Eq. F-1)}$$

where t is the mean groundwater age (yr), λ is the radioactive decay constant 1.21×10^{-4} yr^{-1}; (Clark and Fritz 1997, p. 201), ^{14}A is the measured ^{14}C activity, and $^{14}A_0$ is the assumed initial activity. ^{14}C activities (ages) typically are expressed in percent modern carbon (pmc). A ^{14}C activity of 100 pmc is taken as the ^{14}C activity of the atmosphere in the year 1890, before the natural ^{14}A of the atmosphere was diluted by large amounts of ^{14}C-free carbon dioxide gas from burning fossil fuels (Clark and Fritz 1997, p. 18).

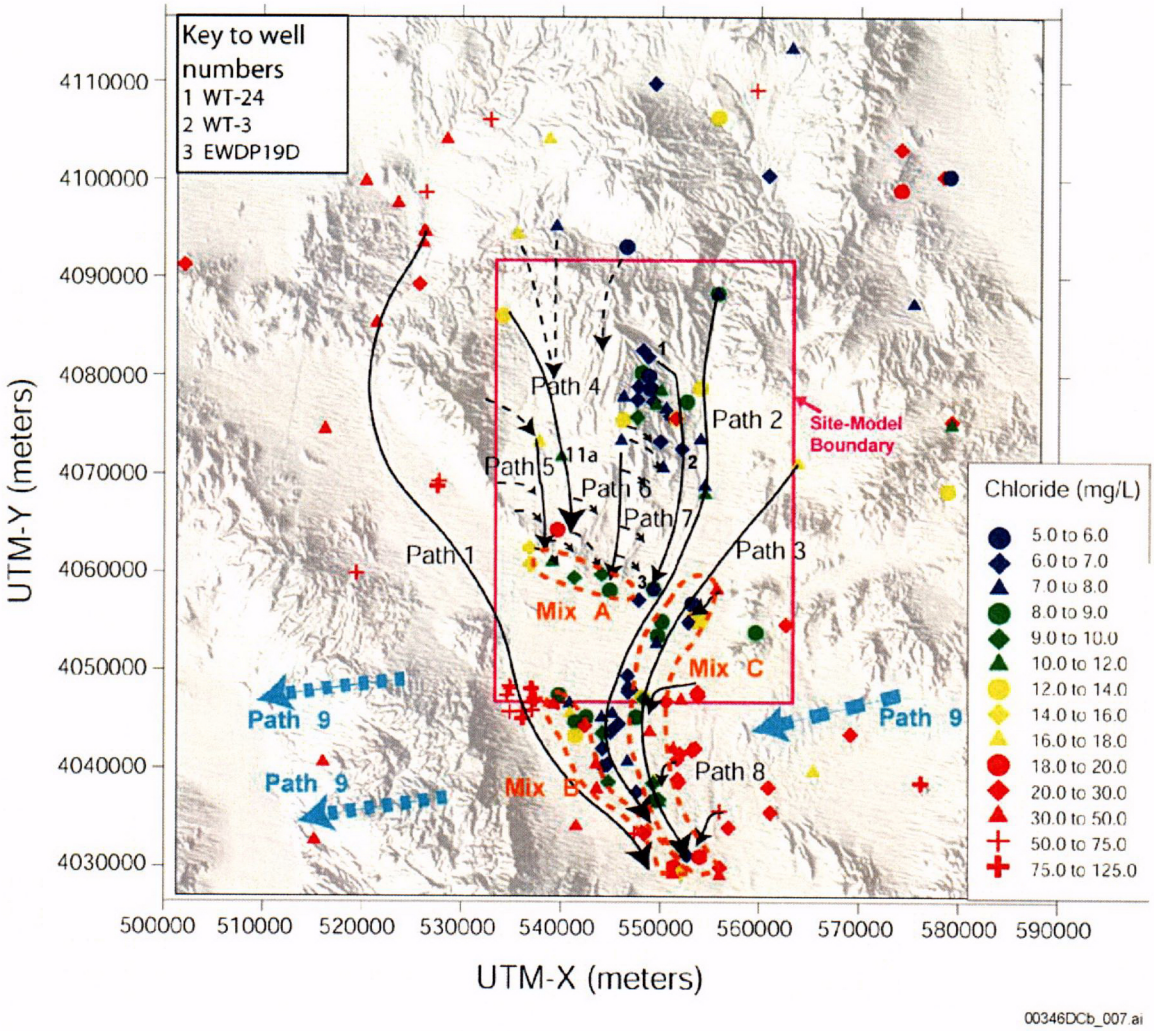

Source: BSC 2003, Figure 62.

NOTE: Chloride values provided as an example.

Figure F-1. Regional Flow Paths Inferred from Hydrochemical and Isotopic Data

Theoretically, the activity of ^{14}C in a groundwater sample reflects the time at which the water was recharged. Unfortunately, precipitation generally is dilute and has a high affinity for dissolution of solid phases in the soil zone, unsaturated zone, and saturated zone. In particular, in the transition from precipitation compositions to groundwater compositions, the concentration of combined bicarbonate and carbonate in the water commonly increases by orders of magnitude (Langmuir 1997, Table 8.7; Meijer 2002). Because bicarbonate is the principal ^{14}C-containing species in most groundwaters, the source of the additional bicarbonate can have a major impact on the "age" calculated from the ^{14}C activity of a given sample. If the source primarily is decaying plant material in an active soil zone, the calculated "age" for the water sample should be close to the true age. In contrast, if the source of the bicarbonate is the dissolution of old (i.e., older than 10^4 yr) calcite with low ^{14}C activity, or oxidation of old organic material, then the calculated age for the sample will be overestimated.

A useful measure of the source of the carbon in a water sample is the $\delta^{13}C$ value of the sample because this value is different for organic materials and calcites. The $\delta^{13}C$ value, in units of per mil, is defined as

$$\delta^{13}C = \left[\frac{\left(^{13}C/^{12}C\right)_{sample}}{\left(^{13}C/^{12}C\right)_{standard}} - 1 \right] \times 1000 \qquad \text{(Eq. F-2)}$$

The standard used for reporting stable carbon isotope measurements is carbon from a belemnite fossil from the Cretaceous Peedee formation in South Carolina (Clark and Fritz 1997, p. 9).

The $\delta^{13}C$ values of plant matter in arid soils generally range from -25 to -13 per mil (Forester et al. 1999, p. 36). Soil waters can also dissolve atmospheric CO_2, which has a $\delta^{13}C$ value of about –8 per mil at Yucca Mountain. Pedogenic carbonate minerals at Yucca Mountain have $\delta^{13}C$ values that generally are between -8 and -4 per mil, although early-formed calcites from deep within Yucca Mountain (from the Exploratory Studies Facility) have $\delta^{13}C$ values greater than 0 per mil (Forester et al. 1999, Figure 16; Whelan et al. 1998, Figure 5). Paleozoic carbonate rocks typically have $\delta^{13}C$ values close to 0 per mil (Clark and Fritz 1997, Figure 5-12).

F.4.3 Delta Carbon-13 Data and Discussion

The areal distributions of $\delta^{13}C$ values are shown in Figure F-2. Excluding data from borehole UE-25 p#1, where groundwater has $\delta^{13}C$ values of –2.3 per mil in the carbonate aquifer and -4.2 per mil in the volcanic aquifer, the $\delta^{13}C$ values of groundwater in the volcanic aquifer at Yucca Mountain vary between -14.4 per mil at borehole USW UZ-14 to -4.9 per mil at borehole USW H-3. Although patterns are complex on a borehole-by-borehole basis, groundwater in the northernmost part of Yucca Mountain is generally lighter (i.e., more negative values) in $\delta^{13}C$ than groundwaters toward the central and southern parts of the mountain.

North of Yucca Mountain, groundwater $\delta^{13}C$ values are generally considerably heavier (i.e., more positive values) than the groundwater $\delta^{13}C$ values found at Yucca Mountain. This suggests that groundwater at Yucca Mountain is not simply groundwater that flowed southward from recharge areas to the north (e.g., Timber Mountain). Only groundwater from borehole ER-EC-07 in Beatty Wash has a $\delta^{13}C$ within the range of values found at Yucca Mountain, Solitario Canyon Wash, and Crater Flat (borehole USW VH-1). The most likely explanation for these data is that there is substantial local recharge at Yucca Mountain and areas immediately to the north (e.g., Yucca Wash and Pinnacles Ridge).

The $\delta^{13}C$ values of groundwater in Nye County Early Warning Drilling Program (EWDP) boreholes at the southern edge of Crater Flat are similar in value to those in groundwaters from boreholes in the southern portion of Yucca Mountain. Thus, these data provide little evidence of water-rock interaction (e.g., calcite dissolution) between groundwaters from these two areas. The westernmost Nye County EWDP boreholes appear to sample groundwater from carbonate rocks with relatively large $\delta^{13}C$ values.

The $\delta^{13}C$ values of groundwater near Fortymile Wash generally increase from north to south within the site-model area, although local reversals in this trend are evident. The north-south variations in groundwater $\delta^{13}C$ values near Fortymile Wash are similar to those observed in groundwaters from boreholes on Yucca Mountain (Figure F-2). This may reflect a major Yucca Mountain component in groundwaters in Fortymile Wash. Alternatively, it reflects similar processes operating on groundwater from north to south. Groundwater in Jackass Flats, and some groundwater at Amargosa Valley, has relatively light $\delta^{13}C$ values, despite the proximity of the Amargosa Valley group samples to groundwater near the gravity fault with considerably higher $\delta^{13}C$ values.

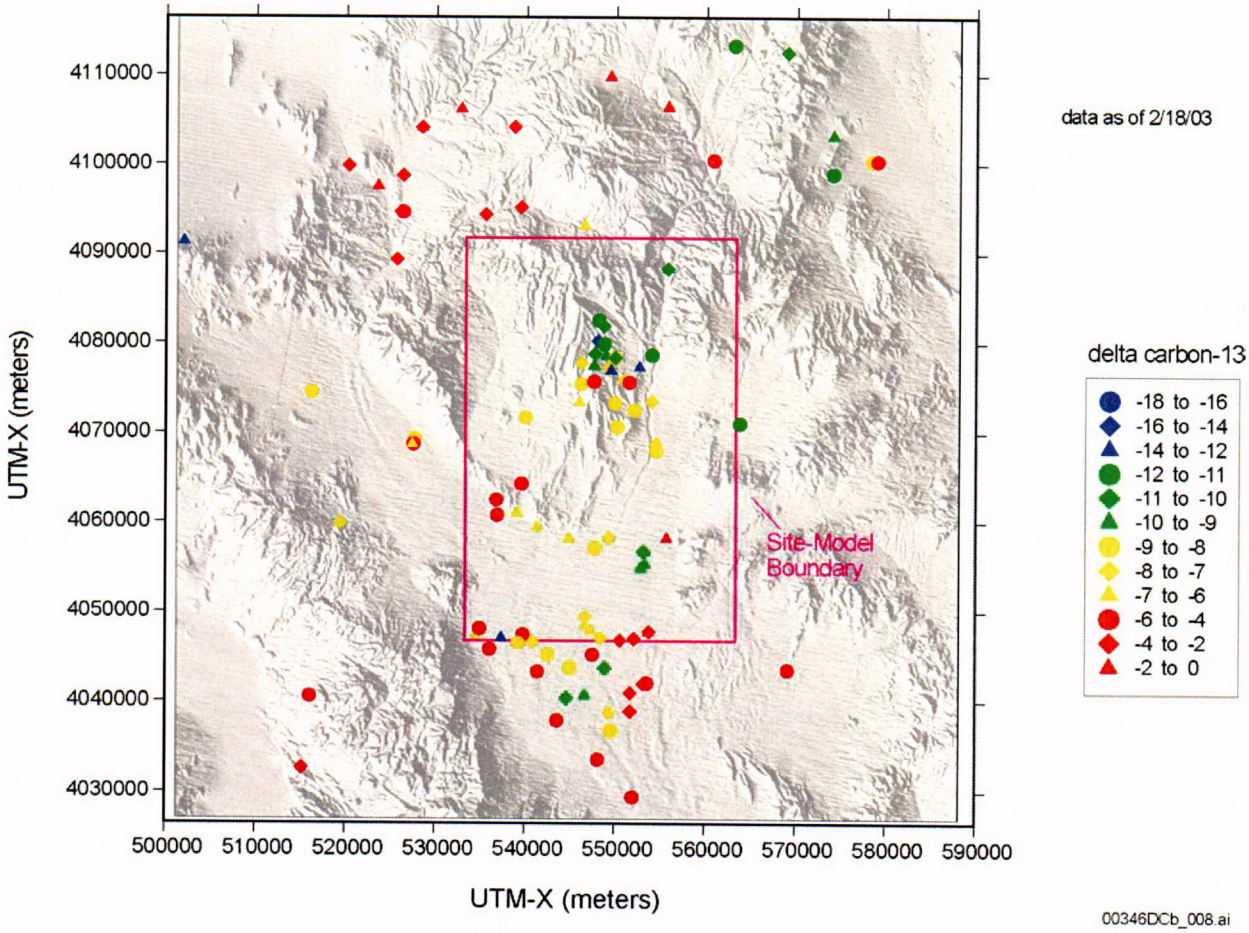

Source: BSC 2003, Figure 27.

Figure F-2. Areal Distribution of Delta Carbon-13 in Groundwater

F.4.4 ^{14}C Activity Data and Discussion

The areal distribution of ^{14}C activity is shown in Figure F-3. Excluding data from borehole UE-25 p#1, which has a ^{14}C activity of 2.3 pmc in the carbonate aquifer and 3.5 pmc in the volcanic aquifer, the ^{14}C activity of groundwater at Yucca Mountain ranges from 10.5 pmc at borehole USW H-3 to 27 pmc at borehole USW WT-24 in northern Yucca Mountain. Groundwater at the eastern edge of Crater Flat near Solitario Canyon has some of the lowest ^{14}C activities of groundwater in the map area, with values as low as 7.3 pmc at borehole USW

WT-10 and 10 pmc in a sample from borehole USW H-6. Groundwater ^{14}C activities are slightly higher farther to the west in Crater Flat at borehole USW VH-1 (12 pmc). Groundwater samples collected from several Nye County EWDP boreholes in the southern Yucca Mountain group to the south of borehole USW VH-1 had similar ^{14}C activities. Groundwater samples collected from boreholes NC-EWDP-2D, NC-EWDP-19P, and some zones in NC-EWDP-19D had ^{14}C activities of 20 pmc or more, similar to the ^{14}C activities of groundwater in Dune Wash and Fortymile Wash.

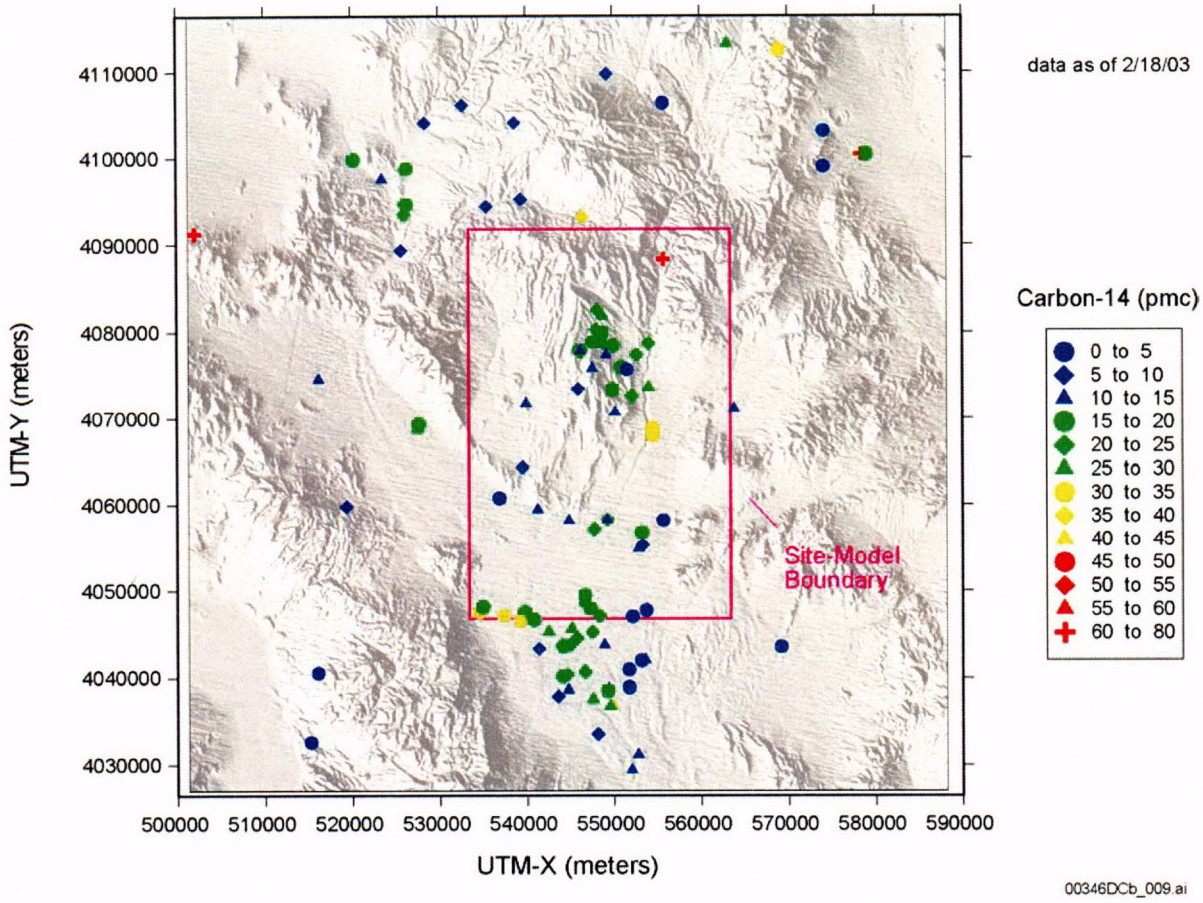

Source: BSC 2003, Figure 28.

Figure F-3. Areal Distribution of ^{14}C in Groundwater

These data do not indicate a clear decrease in ^{14}C activity from north to south along likely flow paths. There is a relatively rapid decrease in ^{14}C activity in groundwater in boreholes between northern and central Yucca Mountain. Conversely, there is little variation in ^{14}C activities between central Yucca Mountain and the Nye County boreholes. As with the $\delta^{13}C$ data, the ^{14}C activity in groundwater samples from boreholes north of Beatty Wash is low. This is additional evidence that groundwater at Yucca Mountain has a large component of local recharge and is not simply groundwater that flowed southward from recharge areas to the north.

Groundwater samples collected near Fortymile Wash had ^{14}C activities that ranged from about 76 pmc at borehole UE-29 a#1 near the northern boundary of the model area to values under

C06

20 pmc near the southern boundary of the model area. The decrease in ^{14}C activities from north to south was irregular (Figure F-3) with the highest value in the northernmost borehole (UE-29 a#1) and the lowest value in borehole NC-EWDP-19D, which is a composite borehole sample. The decreasing trend in ^{14}C values would appear more consistent if data from boreholes between UE-29 a#1 and J-13 were removed. These boreholes have ^{14}C values lower than expected, which may reflect enhanced flow from the Yucca Mountain area into the Fortymile Wash flow path.

F.4.5 ^{14}C Ages of Groundwater

^{14}C Ages of Dissolved Organic Carbon–Groundwater ages can be calculated directly from the ^{14}C activities of dissolved organic carbon if the ^{14}C activity of the recharge water is known. These ages, however, are maximum ages because organic material in the aquifer would contain no ^{14}C (except for newly drilled boreholes that can be contaminated by modern dissolved organic carbon). The carbon-13 activity of dissolved organic carbon is a good indicator of contamination problems if dissolved organic carbon form drilling fluids are present in the sample or if old (potentially isotopically light) organic carbon is being leached from aquifer materials. Thirteen dissolved organic carbon measurements have been made on samples of groundwater in the Yucca Mountain area. Most of the dissolved inorganic carbon ages for these waters are greater than 12,000 yr, but range from 8,000 to 16,000 yr. The youngest dissolved organic carbon and dissolved inorganic carbon radiocarbon ages are for water from upper Fortymile Canyon. These ages show a slight reverse discordance such that the dissolved inorganic carbon ages are slightly younger than the dissolved organic carbon ages (Figure F-4).

^{14}C Ages of Perched Water–Although groundwater ages based on inorganic carbon are susceptible to modification through water-rock reactions, various observations indicate that the ^{14}C ages of the perched-water samples from boreholes on Yucca Mountain do not require substantial correction for the dissolution of carbonate. First, the ratios of $^{36}Cl/Cl$ of the perched-water samples are similar to those expected for their uncorrected ^{14}C age, based on reconstructions of $^{36}Cl/Cl$ ratios in precipitation throughout the late Pleistocene and Holocene from pack-rat midden data (Plummer et al. 1997, Figure 3; DTN: LAJF831222AQ97.002; DTN: GS950708315131.003; DTN: GS960308315131.001). Second, Winograd et al. (1992, Figure 2) presented data from calcite deposits that indicated the $\delta^{18}O$ values in precipitation during the Pleistocene were, on average, 1.9 per mil more depleted during pluvial periods compared to interpluvial periods. The $\delta^{18}O$ values of the perched-water samples generally are more depleted than pore-water samples from the shallow unsaturated zone at Yucca Mountain by more than 1.0 per mil (BSC 2003, Figure 48). This consistent difference suggests that, at some boreholes, the perched water may contain a substantial component of Pleistocene-age water.

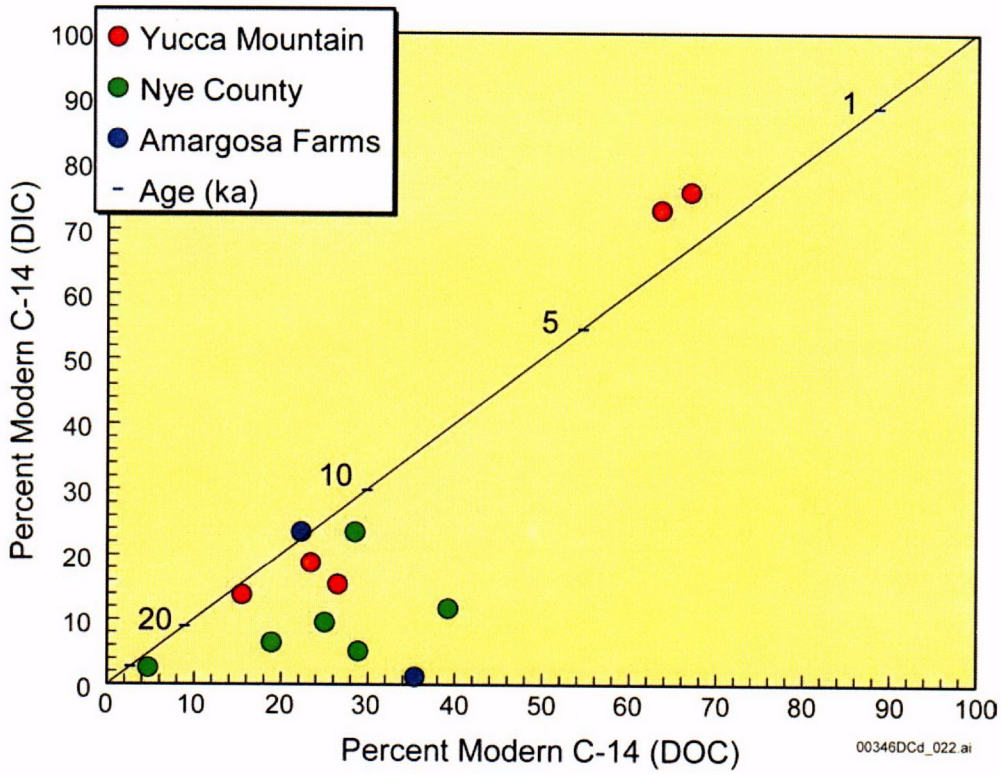

Source: Peters 2003, Slide 36 of 68.

Note: The numbers on the diagonal line are groundwater ages in thousands of years, calculated assuming $^{14}A_0$ is 100 pmc. DOC = dissolved organic carbon; DIC = dissolved inorganic carbon; ka = thousand years.

Figure F-4. Comparison of Observed Dissolved Organic and Inorganic ^{14}C Ages in Groundwaters in the Vicinity of Yucca Mountain

C07

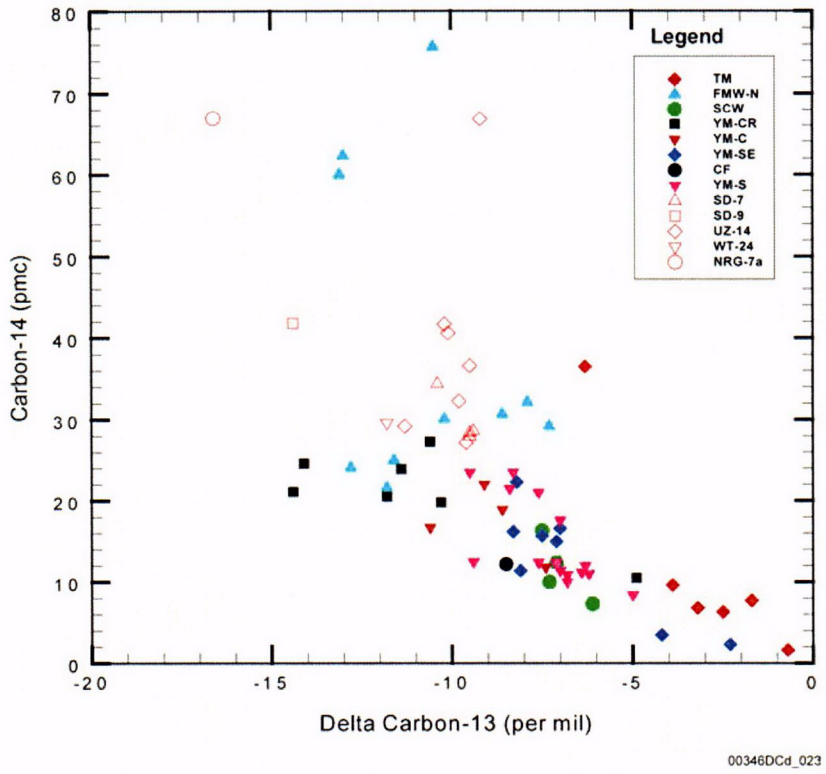

Source: BSC 2003, Figure 45.

NOTE: Solid symbols are groundwater; open symbols are perched water. Location abbreviations in the legend stand for the following: TM = Timber Mountain, FMW-N = Fortymile Wash – North, YM-CR = Yucca Mountain – Crest, YM-C = Yucca Mountain – Central, YM-SE = Yucca Mountain – Southeast, YM-S = Yucca Mountain – South, CF = Crater Flat, and SCW = Solitario Canyon Wash.

Figure F-5. ^{14}C Activity Versus δ^{13}Carbon of Perched Water and Groundwater Near Yucca Mountain

^{14}C Ages of Groundwater Based on Dissolved Inorganic Carbon–Values for $\delta^{13}C$ and ^{14}C in perched waters and groundwaters from the Yucca Mountain area are plotted in Figure F-5. Excluding perched-water samples and the Fortymile Wash area (FMW-N; a group of boreholes east and northeast of Yucca Mountain), the $\delta^{13}C$ and ^{14}C values reported for the groundwater samples are negatively correlated. In the absence of chemical reactions or mixing, waters moving from source areas to Yucca Mountain should experience no change in $\delta^{13}C$, but the ^{14}C activity should decrease with time. If waters infiltrating into the source area have approximately constant $\delta^{13}C$ values, data points for waters infiltrated at different times would form a vertical trend in Figure F-5. The fact that the data points do not form a vertical trend suggests that the $\delta^{13}C$ of waters infiltrated at the source areas are not constant or that chemical reactions or mixing have affected the carbon isotope values. If waters that infiltrate into the source areas have randomly variable $\delta^{13}C$ ratios, then a random relation between $\delta^{13}C$ and ^{14}C values would be expected. Rather, the $\delta^{13}C$ and ^{14}C values for Yucca Mountain and Crater Flat groundwaters are well correlated, suggesting a relationship between these parameters.

The $\delta^{13}C$ values of infiltrating waters reflect the types of vegetation present at the infiltration point. The $\delta^{13}C$ values of modern water that infiltrate in cooler climates (or at higher elevations) are more negative than the values for water that infiltrates in warmer climates (or at lower

elevations) (Quade and Cerling 1990, p. 1,550). This relation should produce a positive correlation in Figure F-5 because the older samples (i.e., lowest pmc) would tend to have the most negative $\delta^{13}C$ (i.e., they infiltrated when the climate was cooler than it is now). Because the observed correlation in the groundwater values is negative, the primary cause of the correlation involves other processes.

Possible explanations for the observed trend are calcite dissolution and mixing with groundwater from the carbonate aquifer. Both of these processes tend to introduce dissolved inorganic carbon with heavy $\delta^{13}C$ and little ^{14}C. This explanation assumes that points on the regression line are of the same age, but that the water dissolved different amounts of calcite. However, the scatter of points about the regression line could be due to inclusion of samples of different ages.

^{14}C ages, based on inorganic carbon, were calculated for locations at Yucca Mountain where groundwater had been identified (from anomalously high $^{234}U/^{238}U$ ratios) as originating mostly from local recharge (Paces et al. 1998). Corrections were also made to the ^{14}C ages of groundwater from several locations for which $^{234}U/^{238}U$ activity ratios were not measured, but which may contain substantial fractions of local Yucca Mountain recharge (based on proximity to groundwater with high $^{234}U/^{238}U$ activity ratios). As the local recharge would most likely have compositions close to that of perched water, perched water was used as a starting composition.

To calculate the correction factor, q, for the dissolution of calcite (i.e., radiometrically "dead" inorganic carbon), the bicarbonate concentrations of the groundwaters were compared with the bicarbonate concentration of perched water. The difference was attributed to dissolution of calcite. The corrections assume that dissolved inorganic carbon of local recharge (as $mDIC_{rech}$) varies between 128.3 and 144 mg/L bicarbonate (HCO_3^-), based on values measured in perched water at Yucca Mountain (Yang et al. 1996). The correction factor ranges from 0.74 at borehole UE-25 WT #12 to 1.0 at several other boreholes (Table F-1). Corrected ^{14}C ages for groundwater range from 11,430 years at borehole UE-25 WT #3 to 16,390 years at borehole UE-25 WT #12 (Table F-1). These calculations show that only minor corrections to the groundwater ^{14}C ages are necessary for samples located along the estimated flow path from the repository.

Table F-1. Chemistry and Ages of Groundwaters from Seven Boreholes at Yucca Mountain

Borehole	$^{234}U/^{238}U$ Activity Ratio	^{14}C Activity (pmc)	DIC, as HCO_3, (mg/L)	Log P_{CO2} (atm)	Log $(IAP/K_{cal})^a$	Factor q	Corrected ^{14}C age (years)	Uncorrected ^{14}C age (years)
USW G-2	7 to 8	20.5	127.6	-2.352	-0.791	1	13,100	13,100
UE-25 WT #17	7 to 8	16.2	150.0	-1.958	-1.175	0.86 to 0.96	13,750 to 14,710	15,040
UE-25 WT #3	7 to 8	22.3	144.3	-2.413	-0.515	0.89 to 1.0	11,430 to 12,380	12,400
UE-25 WT #12	7 to 8	11.4	173.9	-2.327	-0.313	0.74 to 0.83	15,430 to 16,390	17,950
UE-25 C #3	7 to 9	15.7	140.2	-2.458	-0.319	0.92 to 1.0	14,570 to 15,300	15,300
UE-25 B #1 (Tcb) [b]	---	18.9	152.3	-1.892	-0.757	0.84 to 0.95	12,350 to 13,300	13,770
USW G-4	---	22.0	142.8	-2.490	-0.305	0.90 to 1.0	11,630 to 12,510	12,500

NOTE: DIC = dissolved inorganic carbon.

[a] Log (IAP/K_{cal}) is the calcite saturation index. Negative values indicate undersaturation with calcite.

[b] The sample from borehole UE-25 B#1 came from the Bullfrog Tuff (Tcb).

F.4.6 Evaluation of Groundwater Velocities in the Yucca Mountain Region

Groundwater velocities were estimated along various flow path segments using the groundwater ^{14}C activities along the flow path. Measured ^{14}C activities at the upgradient borehole were adjusted to account for decrease in ^{14}C activity that results from water-rock interactions between boreholes, as identified by PHREEQC mixing and chemical reaction models (described in BSC 2003). The adjustment is necessary to distinguish between the decrease in ^{14}C activity caused by water-rock interaction and the decrease in activity due to transit time between the boreholes. After determining the transit time between boreholes, linear groundwater velocities were determined by dividing the distance between the boreholes by the transit time.

The transit time between boreholes was calculated from the radioactive decay equation for ^{14}C (Equation F-1). A variety of methods have been used to estimate the value of $^{14}A_0$ for use with the radioactive decay law (Clark and Fritz 1997, Chapter 8). One simple method, which can be used to correct for the effects of calcite (or dolomite) dissolution when the downgradient groundwater evolves from a single upgradient source, is to compare the total dissolved inorganic carbon in the upgradient borehole ($m_{DIC\text{-}U}$) with the dissolved inorganic carbon of the downgradient groundwater ($m_{DIC\text{-}D}$) (Clark and Fritz 1997, p. 209):

$$q_{DIC} = \frac{m_{DIC\text{-}U}}{m_{DIC\text{-}D}} \qquad \text{(Eq. F-3)}$$

The value of q_{DIC} represents the fraction of dissolved inorganic carbon in the downgradient water that originated from the upgradient borehole, with the remainder acquired from water-rock-gas interactions. Therefore, the initial value of $^{14}A_0$ is the product of q_{DIC} and the measured ^{14}C activity at the upgradient borehole ($^{14}A_U$):

$$^{14}A_0 = {}^{14}A_U \times q_{DIC} \quad \text{(Eq. F-4)}$$

This method assumes that after infiltration reaches the saturated zone, the water is effectively isolated from further interaction with carbon dioxide gas in the unsaturated zone and that any downgradient increases in the dissolved inorganic carbon of the groundwater are a result of interactions with carbon-bearing minerals. The ^{14}C content of these minerals is assumed to be depleted, which is probably the case because most saturated zone calcite was formed during a 10-million-year-old hydrothermal event or during deposition under unsaturated conditions when the water table was lower than today (Whelan et al. 1998). Thus, although the proportions of dissolved carbon dioxide gas, bicarbonate, and carbonate may change with pH as the groundwater interacts with the rock, the total dissolved inorganic carbon is fixed unless the groundwater reacts with calcite. This method would not account for interactions between groundwater and calcite after the groundwater became saturated with calcite, nor would it account for the effects of groundwater mixing. This method was applied to obtain preliminary estimates where the upgradient groundwater was undersaturated with calcite and mixing was not considered an important process (based on the PHREEQC inverse models).

For flow path segments where PHREEQC inverse models indicate that downgradient groundwater evolves from a single upgradient borehole, the value of $^{14}A_U$ is simply groundwater ^{14}A at the upgradient borehole, and q_{DIC} is computed as

$$q_{DIC} = \frac{DIC_U}{DIC_U + DIC_{carbonate}} \quad \text{(Eq. F-5)}$$

where DIC_U is the dissolved inorganic carbon at the upgradient borehole, and $DIC_{carbonate}$ is the amount of carbon contributed by water-rock interactions involving carbonate rocks.

For flow path segments where the PHREEQC inverse models identified mixing as having an important affect on the downgradient groundwater chemistry, the values of $^{14}A_U$ and q_{DIC} are calculated as

$$^{14}A_U = \frac{f_1 {}^{14}A_1 DIC_1 + f_2 {}^{14}A_2 DIC_2 + \cdots + f_i {}^{14}A_i DIC_i}{f_1 DIC_1 + f_2 DIC_2 + \cdots + f_i DIC_i} \quad \text{(Eq. F-6)}$$

and

$$q_{DIC} = \frac{f_1 DIC_1 + f_2 DIC_2 + \cdots + f_i DIC_i}{f_1 DIC_1 + f_2 DIC_2 + \cdots + f_i DIC_i + DIC_{carbonate}} \quad \text{(Eq. F-7)}$$

where f_1 to f_i are the fractions of various upgradient components in the mixture and the subscripts 1, 2, ..., i indicate the component in the mixture. The equations do not consider the

effects of CO_2 degassing, dissolution, or calcite precipitation. This simplification is acceptable because the fractionation factor for ^{14}C is small (Clark and Fritz 1997) and the ^{14}C in the CO_2 or calcite exiting the groundwater should leave the ^{14}C in the groundwater relatively unchanged. Gas dissolution by the groundwater should not occur in most instances because the log pCO_2 of the groundwater is higher than that of the overlying unsaturated zone (BSC 2003, Section 6.5.5).

Flow path segment UE-25 WT#3 to NC-EWDP-19D–Results from the PHREEQC inverse models (BSC 2003, Section 6.5.8) indicate that groundwater sampled from various zones in borehole NC-EWDP-19D could have evolved from groundwater in the vicinity of UE-25 WT#3. Transit times were calculated using the dissolved inorganic carbon of groundwater at borehole UE-25 WT#3 and PHREEQC estimates of the carbon dissolved by this groundwater as it moves toward various zones at borehole NC-EWDP-19D (Table F-2). Groundwater in the composite borehole and alluvial groundwaters requires approximately 1,000 to 2,000 years to travel between boreholes UE-25 WT#3 and NC-EWDP-19D, a distance of approximately 15 km. This equates to linear groundwater velocities of approximately 7.5 to 15 m/yr. The groundwater in the deeper alluvial zones (Zones 3 and 4) of borehole NC-EWDP-19D requires approximately 1,500 to 3,000 years and therefore travels at a linear groundwater velocity of 5 to 10 m/yr. In contrast, the transit times calculated for groundwater from shallow Zones 1 and 2 have transit times that range from 0 to about 350 years. Most of the calculated groundwater transit times were negative, indicating that the differences between ^{14}C activities in the groundwater at borehole USW WT-3 and these zones in borehole NC-EWDP-19D were too small, and that the uncertainty in dissolved inorganic carbon reactions estimated by PHREEQC too large, to adequately resolve the transit times. Using the upper age of 350 years, groundwater flow from borehole UE-25 WT#3 to Zones 1 and 2 in borehole NC-EWDP-19D is about 40 m/yr. This relatively high velocity may indicate that some of the shallow groundwater at borehole UE-25 WT#3 moves along major faults (e.g., the Paintbrush Canyon fault).

Flow path segment USW WT-24 to UE-25 WT#3–Transit times were calculated using the dissolved inorganic carbon of groundwater at borehole USW WT-24 and PHREEQC estimates of the carbon dissolved by the groundwater as it moves toward borehole UE-25 WT#3 (Table F-3). Transit times based on the PHREEQC models range from 0 to slightly over 1,000 years. The transit time estimate based on the differences in dissolved inorganic carbon of groundwater at boreholes USW WT-24 and UE-25 WT#3 is 216 years. Using this estimate of transit time and a linear distance between boreholes USW WT-24 and UE-25 WT#3 of 10 km, the linear groundwater velocity is 46 m/yr. The longest transit time (1,023 years) results in a groundwater velocity of about 10 m/yr.

Table F-2. Calculated Groundwater Transport Times between Borehole USW WT-3 and Various Depth Zones in Borehole NC-EWDP-19D

Model Number [a]	Open Borehole	Alluvium Composite	Zone 1 [b]	Zone 2	Zone 3	Zone 4
1	2332	2048	0	0	2151	2802
2	2275	2535	0	0	2521	2802
3	2325	2334	0	0	2894	2800
4	2325	2535	359	70	2968	2800
5	2332	2048	0	0	2941	2798
6	2273	2049	0	295	2149	2798
7	2328	2049	0	0	2149	---
8	2275	2501	359	0	2521	---
9	2328	2050	0	0	2521	---
10	2324	2050	186	0	2521	---
11	2273	---	305	---	3027	---
12	2325	---	0	---	---	---
13	2325	---	0	---	---	---
DIC estimate [c]	866	1063	0	188	1601	1681

NOTE: DIC = dissolved inorganic carbon. "---" means that no model was produced beyond those indicated by the numerical values.

[a] Model number refers to various PHREEQC models produced for that zone using groundwater from USW WT-3 as the source groundwater.

[b] Zones 1 to 4 are all isolated zones in alluvium. When negative transit times were calculated, the value was set to 0 years.

[c] DIC estimate refers to the transit time estimate made from the measured dissolved inorganic carbon at borehole USW WT-3 and that particular zone in borehole NC-EWDP-19D.

Table F-3. Calculated Groundwater Transport Times between Boreholes USW WT-24 and USW WT-3

PHREEQC model	Transit time (yr)
1	0
2	555
3	725
4	0
5	0
6	749
7	430
8	717
9	567
10	0
11	1,023
12	883
13	0
DIC estimate	216

NOTE: When negative transit times were calculated, the value was set to 0 years. DIC = dissolved inorganic carbon.

Under ideal circumstances, the decrease in groundwater ^{14}C activities along a flow path can be used to calculate groundwater velocities. The calculation is straightforward when groundwater recharge occurs in a single location and groundwater downgradient from this location does not receive addition recharge or mix with other groundwater. In the Yucca Mountain area, calculating groundwater velocity based on ^{14}C activity is complicated by the possible presence of multiple, distributed recharge areas. If relatively young recharge were added along a flow path, the ^{14}C activity of the mixed groundwater would be higher and the calculated transport times shorter than for the premixed groundwater without the downgradient recharge. Unfortunately, the chemical and isotopic characteristics of the recharge from various areas at Yucca Mountain may not be sufficiently distinct to identify separate sources of local recharge in the groundwater. Conversely, if groundwater from the carbonate aquifer were to mix downgradient with Yucca Mountain recharge, the mixture would have a lower ^{14}C activity than the Yucca Mountain recharge component because of the high carbon alkalinity and low ^{14}C activity of the carbonate aquifer groundwater. However, the presence of groundwater from the carbonate aquifer in the mixture would be recognized because of the distinct chemical and isotopic composition of that groundwater compared with the recharge water, and the effect on the ^{14}C activity of the groundwater mixture could be calculated.

F.4.7 Residence Times

The residence time for water that originates at the repository level and subsequently moves to the accessible environment is calculated as the sum of the average age of perched water corrected for travel time from the surface to the perched water horizon and the transit times calculated for water moving from USW WT-24 to the accessible environment. The ages calculated for perched water range from 7,000 to 11,000 yr based on the ^{14}C activities of perched water samples assuming $^{14}A_0$ equals 100 pmc (BSC 2003). The travel times calculated for water infiltrated at the surface and percolated to the perched water zones range from 1,000 to 4,000 yr. Most of this travel time is taken up in the bedded tuffs of the PTn. Thus, the residence time for water in the perched zones ranges from 3,000 to 10,000 yr. A single sample from borehole NRG-7a, and one of several samples from UZ-14, had much younger ^{14}C ages of about 3,300 yr. These samples were obtained with bailers instead of pumps. They are waters that stagnated in the borehole for some period of time. Therefore, it is more likely that they were compromised by mixing with atmospheric gases than by waters pumped from the formation. If these samples were included, the water residence time in the perched zones would range from 0 to 10,000 yr.

When the residence time of water in the perched zones is combined with the estimates of travel time between USW WT-24 and the accessible environment, a range of total residence times of 0 to 10,000 yr is obtained. The low end of this range is very model dependent (PHREEQC) and likely an underestimate. When compared to the range in ages (8,000 to 16,000 yr) calculated for saturated zone waters from ^{14}C measurements on dissolved organics, the 0 to 10,000 yr range also appears to underestimate the true range in residence times unless saturated zone waters are on the order of 8,000 yr old when they reach Yucca Mountain from upgradient locations. The strong evidence for local recharge (i.e., $^{234}U/^{238}U$, delta ^{13}C, and ^{14}C data) suggests this scenario is not correct. Thus, the ^{14}C analysis of residence times appears to underestimate the residence times for water between the repository and the accessible environment.

F.5 REFERENCES

F.5.1 Documents Cited

BSC (Bechtel SAIC Company) 2003. *Geochemical and Isotopic Constraints on Groundwater Flow Directions and Magnitudes, Mixing, and Recharge at Yucca Mountain.* ANL-NBS-HS-000021 REV 01A. Las Vegas, Nevada: Bechtel SAIC Company. ACC: MOL.20030604.0164.

Clark, I.D. and Fritz, P. 1997. *Environmental Isotopes in Hydrogeology.* Boca Raton, Florida: Lewis Publishers. TIC: 233503.

Forester, R.M.; Bradbury, J.P.; Carter, C.; Elvidge-Tuma, A.B.; Hemphill, M.L.; Lundstrom, S.C.; Mahan, S.A.; Marshall, B.D.; Neymark, L.A.; Paces, J.B.; Sharpe, S.E.; Whelan, J.F.; and Wigand, P.E. 1999. *The Climatic and Hydrologic History of Southern Nevada During the Late Quaternary.* Open-File Report 98-635. Denver, Colorado: U.S. Geological Survey. TIC: 245717.

Langmuir, D. 1997. *Aqueous Environmental Geochemistry.* Upper Saddle River, New Jersey: Prentice Hall. TIC: 237107.

Meijer, A. 2002. "Conceptual Model of the Controls on Natural Water Chemistry at Yucca Mountain, Nevada." *Applied Geochemistry, 17,* ([6]), 793-805. [New York, New York]: Elsevier. TIC: 252808.

Paces, J.B.; Ludwig, K.R.; Peterman, Z.E.; Neymark, L.A.; and Kenneally, J.M. 1998. "Anomalous Ground-Water 234U/238U Beneath Yucca Mountain: Evidence of Local Recharge?" *High-Level Radioactive Waste Management, Proceedings of the Eighth International Conference, Las Vegas, Nevada, May 11-14, 1998.* Pages 185-188. La Grange Park, Illinois: American Nuclear Society. TIC: 237082.

Peters, M.T. 2003. *Status of Ongoing Testing.* Presented to: Nuclear Waste Technical Review Board, June 14, 2003. 68 pages. Washington, D.C.: Bechtel SAIC Company. ACC: MOL.20030820.0045.

Plummer, M.A.; Phillips, F.M.; Fabryka-Martin, J.; Turin, H.J.; Wigand, P.E.; and Sharma, P. 1997. "Chlorine-36 in Fossil Rat Urine: An Archive of Cosmogenic Nuclide Deposition During the Past 40,000 Years." Science, 277, 538-541. Washington, D.C.: American Association for the Advancement of Science. TIC: 237425.

Quade, J. and Cerling, T.E. 1990. "Stable Isotopic Evidence for a Pedogenic Origin of Carbonates in Trench 14 Near Yucca Mountain, Nevada." Science, 250, 1549-1552. Washington, D.C.: American Association for the Advancement of Science. TIC: 222617.

Reamer, C.W. and Williams, D.R. 2000. Summary Highlights of NRC/DOE Technical Exchange and Management Meeting on Unsaturated and Saturated Flow Under Isothermal Conditions. Washington, D.C.: U.S. Nuclear Regulatory Commission. ACC: MOL.20001128.0206.

Whelan, J.F.; Moscati, R.J.; Roedder, E.; and Marshall, B.D. 1998. "Secondary Mineral Evidence of Past Water Table Changes at Yucca Mountain, Nevada." *High-Level Radioactive Waste Management, Proceedings of the Eighth International Conference, Las Vegas, Nevada, May 11-14, 1998.* Pages 178-181. La Grange Park, Illinois: American Nuclear Society. TIC: 237082.

Winograd, I.J.; Coplen, T.B.; Landwehr, J.M.; Riggs, A.C.; Ludwig, K.R.; Szabo, B.J.; Kolesar, P.T.; and Revesz, K.M. 1992. "Continuous 500,000-Year Climate Record from Vein Calcite in Devils Hole, Nevada." *Science, 258*, 255-260. Washington, D.C.: American Association for the Advancement of Science. TIC: 237563.

Yang, I.C.; Rattray, G.W.; and Yu, P. 1996. Interpretation of Chemical and Isotopic Data from Boreholes in the Unsaturated Zone at Yucca Mountain, Nevada. Water-Resources Investigations Report 96-4058. Denver, Colorado: U.S. Geological Survey. ACC: MOL.19980528.0216.

F.5.2 Data, Listed by Data Tracking Number

GS950708315131.003. Woodrat Midden Age Data in Radiocarbon Years Before Present. Submittal date: 07/21/1995.

GS960308315131.001. Woodrat Midden Radiocarbon (^{14}C). Submittal date: 03/07/1996.

LAJF831222AQ97.002. Chlorine-36 Analyses of Packrat Urine. Submittal date: 09/26/1997.